Supplementary Information

Zeolitization of Fly Ash for Synthesis of Pharmaceutically Important Bis(indolyl)methane Derivatives

Aashima Mahajan[a], Loveleen Kaur Brar*[b] and Manmohan Chhibber*[a]

a) Department of Chemistry and Biochemistry (DCBC), Thapar Institute of Engineering and Technology, Patiala-147004, Punjab, India.

b) Department of Physics and Material Science (DPMS), Thapar Institute of Engineering and Technology, Patiala, 147004-Punjab, India.

E-mail: brarloveleen@thapar.edu, mchhibber@thapar.edu

Table of Contents

S1. Hydrothermal Synthesis of Zeolite A (ZA) at Different Time Durations

The hydrothermal synthesis of zeolite was carried out at different time durations (6, 8, 10, and 12 h), as indicated in the XRD spectra shown in Fig. S1. The XRD pattern of ZA-10H demonstrates that the quartz and mullite peaks of fly ash have disappeared, and the peaks corresponding to ICDD card number 01-089-3859, confirming the formation of Zeolite A. In the XRD pattern for 6 h of hydrothermal treatment (ZA-6H), peaks of Zeolite A appear, along with a hump showing the presence of the amorphous phase. However, after 8 h (ZA-8H), the crystalline phase has developed further with a slight hump, and a pure zeolite phase is achieved after 10 h of treatment. The relative crystallinity, estimated from the integrated areas of the characteristic Zeolite A diffraction peaks, attains a maximum value of 54% for ZA-10H, while the crystallinity values for the other samples are shown in Fig. S2. Further increasing the hydrothermal time to 12 h, there is the formation of a new crystalline phase, identified as Faujasite-Na (ICDD card no. 00-012-0246), along with a decrease in intensity of zeolite A peaks.

Therefore, the ZA-10H was considered the final optimized sample, with the synthesis of pure-phase crystalline zeolite A, and was designated as **ZA**.

$$\text{Crsytallinity \%} = \frac{\text{Area of crystalline peak}}{\text{Area of crystalline and amorphrous peak}} \text{ X } 100$$

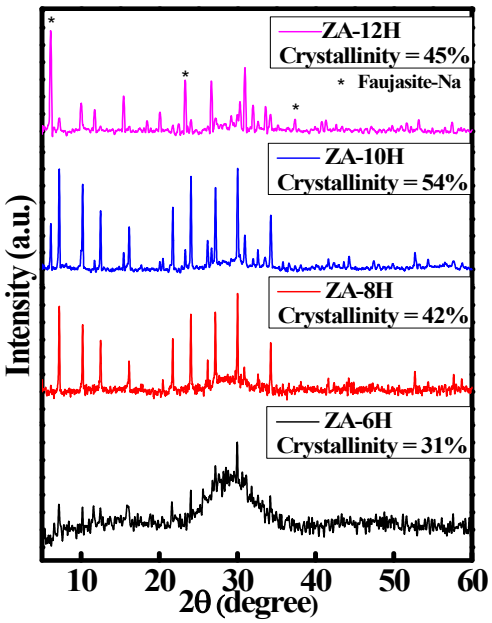

Fig. S1 XRD pattern showing the hydrothermal treatment at different time intervals (6, 8, 10, and 12 hours) for the synthesis of Zeolite A.

S2. Comparative XPS Analysis of ZA and Acid-Treated Zeolite (ZA2/30)

To complement the discussion presented in the main manuscript (Section 3.4), the XPS spectra of zeolite ZA and the acid-treated zeolite (ZA2/30) are provided here. These spectra highlight the changes in atomic % of groups present in each component (Na1s, O1s, C1s, Si2p and Al2p) upon acid treatment. The observations have been documented as Table 2 in the main text.

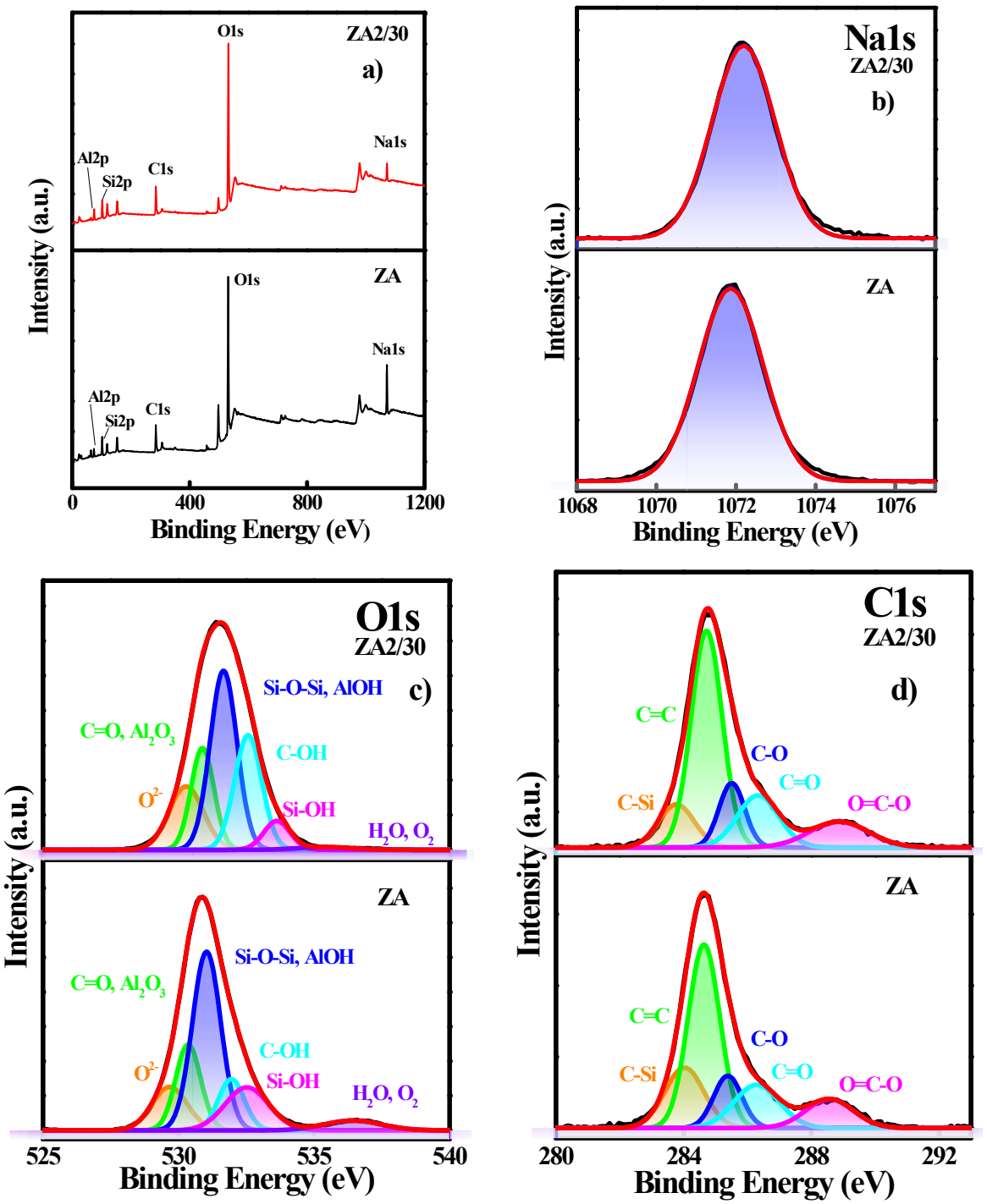

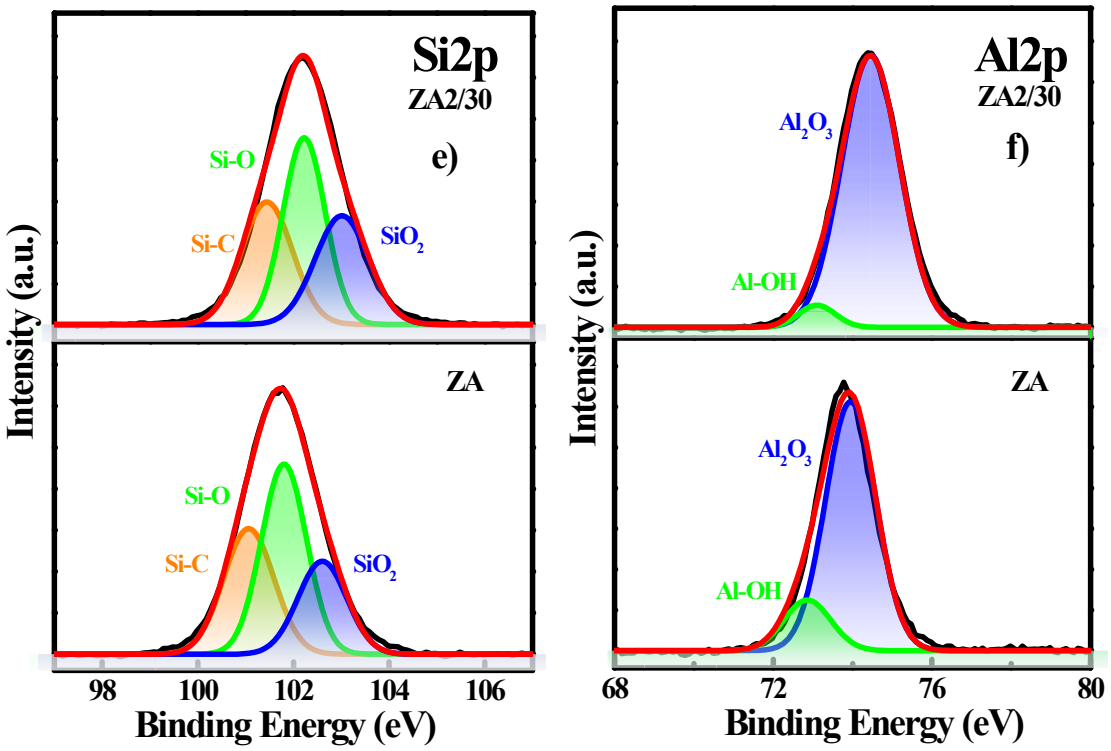

Fig. S2 Comparison of XPS spectra of ZA and acid-treated zeolite (ZA2/30) (a) survey spectra, (b)Na1s, (c) O1s, (d) C1s, (e) Si2p and (f) Al2p.

S3. Comparative NH_3-TPD Analysis of ZA and Acid-Treated Zeolites (ZA2/30, ZA2/90)

The NH_3-TPD deconvoluted spectra of the parent zeolite (ZA) and the acid-treated samples (ZA2/30 and ZA2/90) illustrate the distribution of weak, moderate, and strong acid sites. The deconvolution was performed using the Pearson VII fitting function, and the corresponding R^2 values indicating the goodness of fit are provided in the graphs. The relationship between these acidity profiles and the catalytic performance is discussed in Section 3.4 and summarized in Table 3 of the main manuscript.

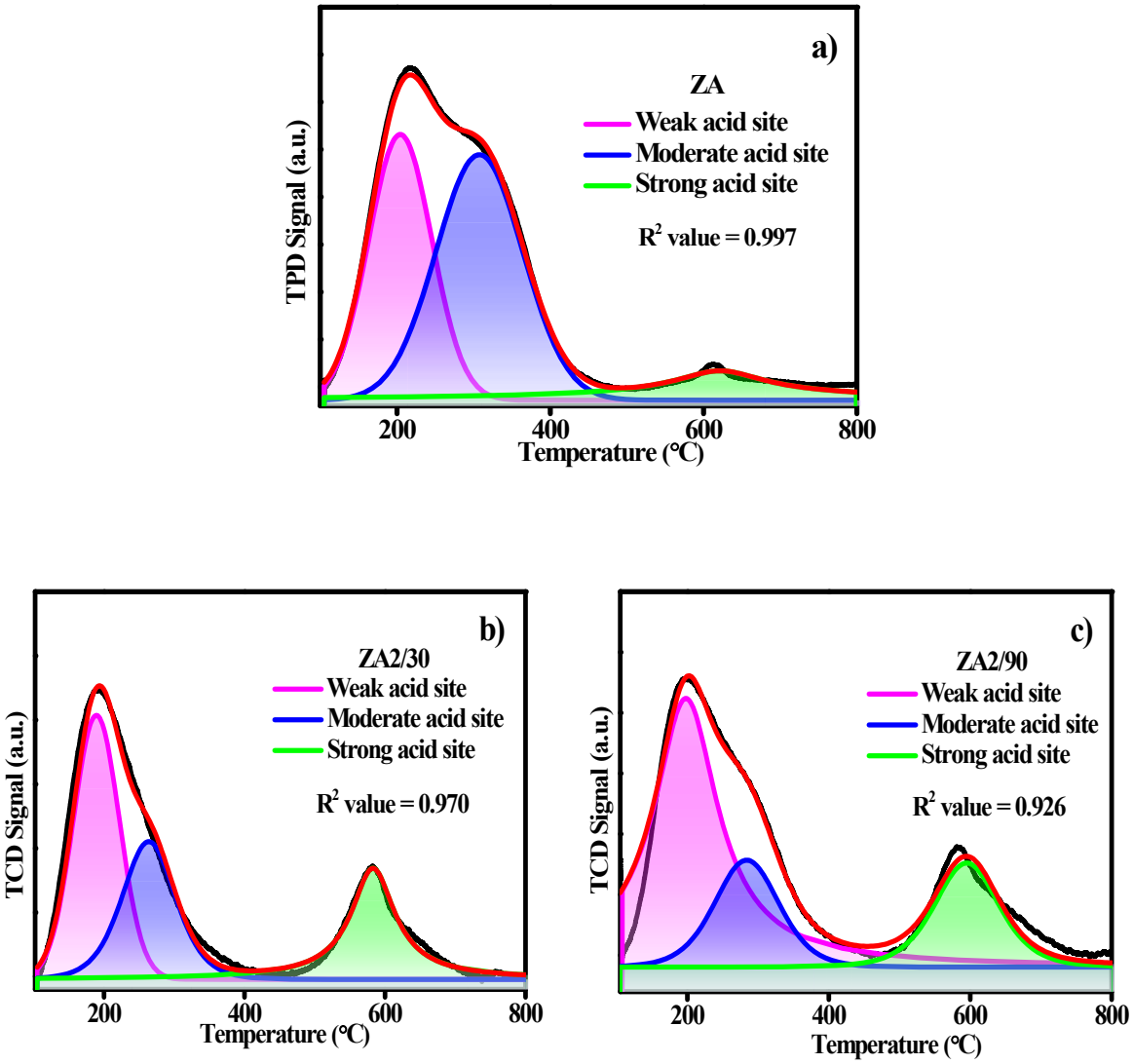

Fig. S3 Deconvoluted NH_3-TPD profiles of (a) ZA (b) ZA2/30 and (c) ZA2/90.

S4. Formula: Calculation of acidity for zeolites (ZA, ZA2/30 and ZA2/90) and TON, TOF using NH_3-TPD data

S4.1 Calculation for acidity in zeolite[1]

1. $$\underset{\text{(Total sites)}}{NH_3 \text{ desorbed (mmol)}} = \frac{\text{Total Area (counts)}}{\text{Calibration Factor (counts/mmol)}}$$

2. $$\text{Acidity (mmol/g)} = \frac{NH_3 \text{ desorbed (mmol)}}{\text{Catalyst weight (g)}}$$

Where:

Calibration factor (counts/mmol) = given in raw data file

Area (counts) = calculated from deconvoluted curve of NH_3-TPD

weight of catalyst = given in raw data file

S4.2 Calculation of TON[2] and TOF[3]

1. $$\text{TON (turnover number)} = \frac{\text{Moles of BIM (compound 3a) formed (moles)}}{NH_3 \text{ desorbed (moles)}}$$

2. $$\text{TOF (turnover frequency, } h^{-1}) = \frac{\text{TON}}{\text{Time for BIM synthesis (compound 3a)}}$$

S5. Characterization Data for the Synthesized Bis(indolyl)methane (BIMs) and their respective ^{1}H and ^{13}C NMR spectra

3,3'-(Phenylmethylene)bis(1H-indole) (3a) Light red solid (68 %); mp: 87- 89 ℃; ^{1}H NMR (400 MHz, $CDCl_3$) δ 7.90 (s, 2H, NH), 7.39 (s, 1H, ArH), 7.37 (s, 1H, ArH), 7.35 (s, 2H, ArH), 7.33 (s, 2H, ArH), 7.28 (d, *J* = 7.1 Hz, 2H, ArH), 7.21 (d, *J* = 7.0 Hz, 1H, ArH), 7.15 (t, *J* = 7.5 Hz, 1H, ArH), 6.99 (t, *J* = 7.4 Hz, 2H), 6.65 (s, 2H, ArH), 5.88 (s, 1H, $(Ar)_3CH$).^{13}C NMR (100 MHz, $CDCl_3$) δ 144.04, 136.73, 128.80, 128.31, 127.12, 126.22, 123.70, 122.01, 120.03, 119.77, 119.30, 111.11, 40.25. HRMS (ESI) calcd for $C_{23}H_{18}N_2$ [M-H]$^-$ 321.1386, found 321.1378.

Fig. S5(a) ^{1}H& ^{13}C NMR spectra of 3,3'-(phenylmethylene)bis(1H-indole)-(**3a)** and LCMS of reaction mixture

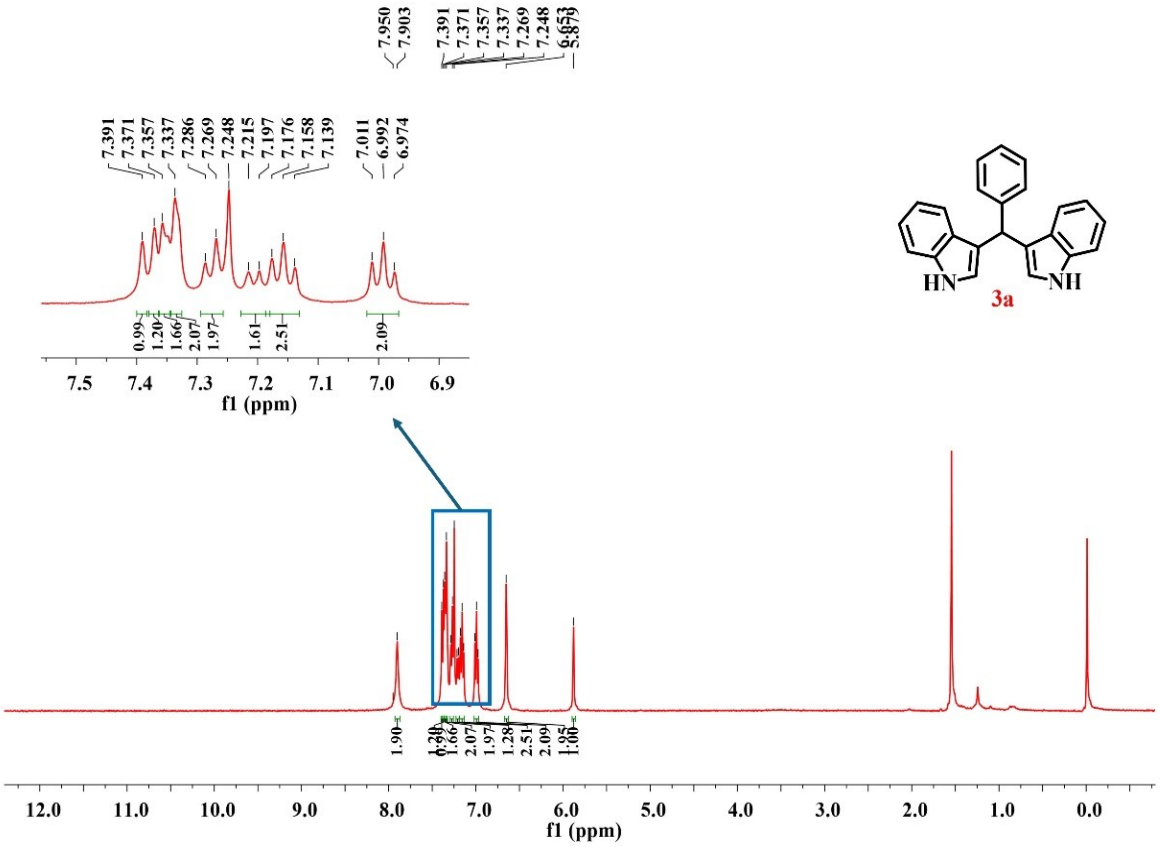

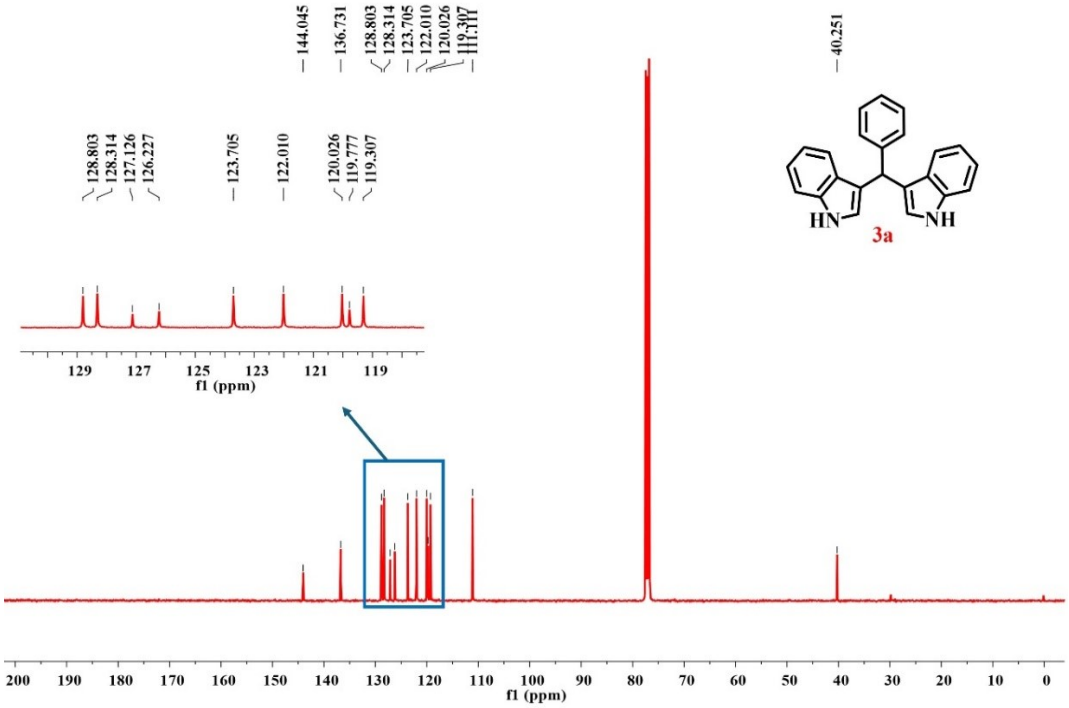

LC–MS analysis of the reaction mixture for compound **3a** was performed to rule out side-product formation. The spectrum clearly shows the molecular ion of **3a** along with its characteristic fragment at *m/z* 206, confirming the selective formation of the desired product.

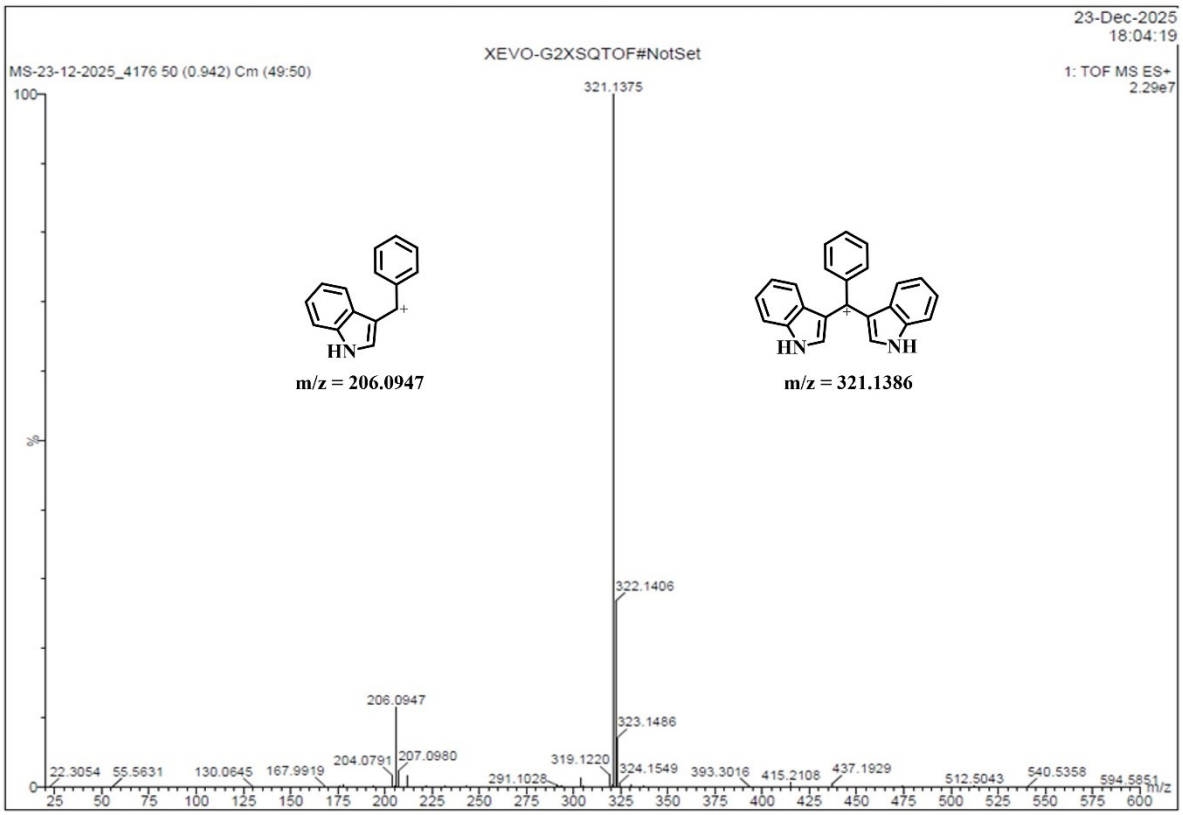

3,3'-((4-Methoxyphenyl)methylene)bis(1H-indole) (3b) orange-red solid (46%); mp: 183-186 °C; ^{1}H NMR (400 MHz, $CDCl_3$) δ 7.86 (s, 2H, NH), 7.44 (d, *J* = 6.36 Hz, 2H, ArH), 7.32 (d, *J* = 6.52 Hz, 2H, ArH), 7.13 (t, *J* = 6.05 Hz, 2H, ArH), 6.98 (t, *J* = 6.0 Hz, 2H, ArH), 6.78 (dd, *J* = 6.0, 1.4 Hz, 1H), 6.74 (dd, *J* = 6.4, 1.4 Hz, 1H), 6.71 – 6.69 (m, 2H, ArH), 6.29 (s, 1H), 5.80 (s, 1H), 5.28 (s, 1H), 3.87 (s, 3H). ^{13}C NMR (100 MHz, $CDCl_3$) δ 146.40, 143.12, 136.72, 129.67, 127.20, 123.44, 122.08, 121.82, 120.03, 119.14, 119.11, 118.99, 110.94, 108.54, 55.89, 32.74. HRMS (ESI) calcd for $C_{24}H_{20}N_2O$ [M-H]$^-$ 351.1491, found [M-H]$^-$ 351.1496.

Fig. S5(b) ^{1}H and ^{13}C NMR spectra of 3,3'-((4-methoxyphenyl)methylene)bis(1H-indole) **(3b)**

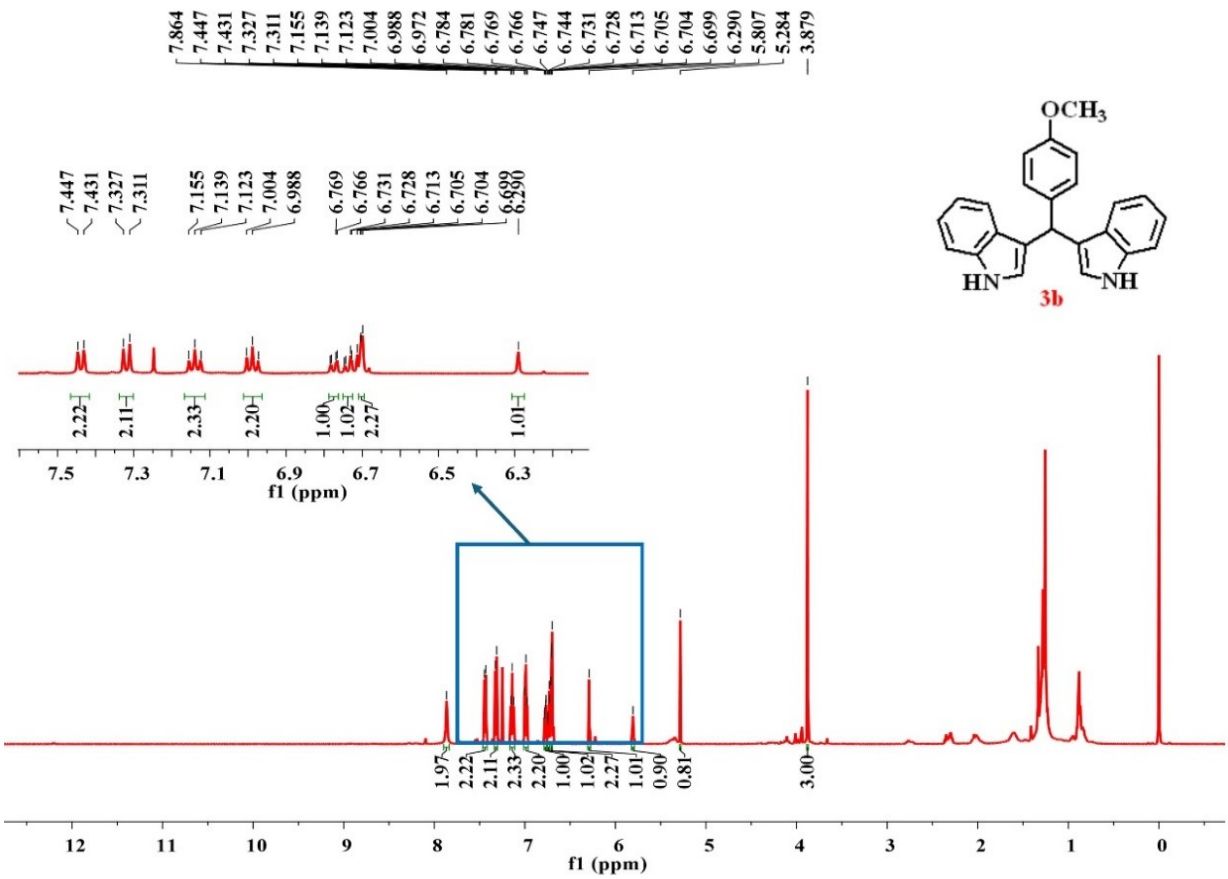

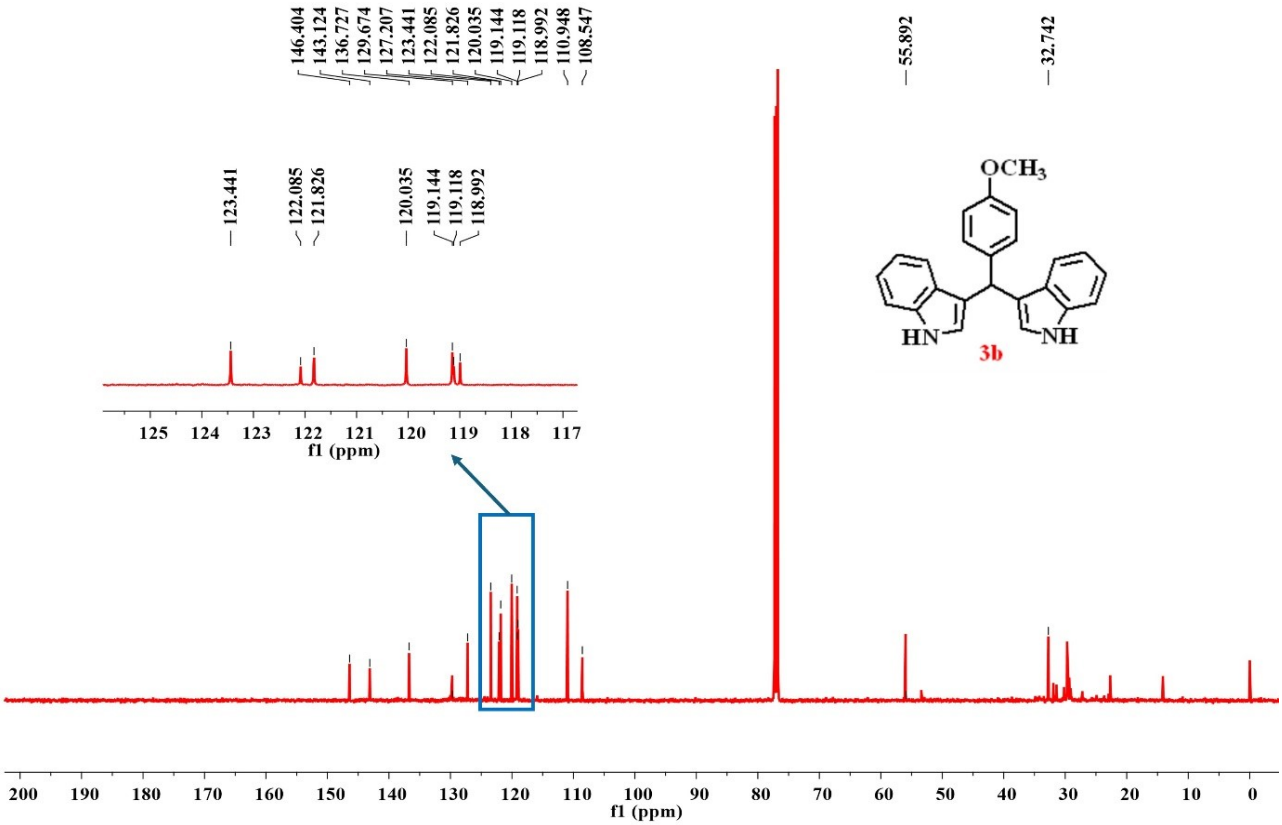

3,3'-((4-Chlorophenyl)methylene)bis(1H-indole) (3c) Red solid (63%); mp:109-113 °C; ^{1}H NMR (400 MHz, $CDCl_3$) δ 7.92 (s, 2H, NH), 7.35 (dd, *J* = 6.4, 2.4 Hz, 4H, ArH), 7.27- 7.22 (m, 4H, ArH), 7.17 (t, *J* = 6.2 Hz, 2H, ArH), 7.00 (t, *J* = 6.0 Hz, 2H, ArH), 6.63 (s, 2H¸ArH), 5.85 (s, 1H, $(Ar)_3CH$). ^{13}C NMR (100 MHz, $CDCl_3$) δ 142.56, 136.69, 131.79, 130.07, 128.35, 126.89, 123.58, 122.07, 119.81, 119.35, 119.21, 111.10, 39.62. HRMS (ESI) calcd for $C_{23}H_{17}ClN_2$ $[M-H]^-$ 355.0996, found $[M-H]^-$ 354.9932.

Fig. S5(c). ^{1}H and ^{13}C NMR spectra of 3,3'-((4-chlorophenyl)methylene)bis(1H-indole)-**(3c).**

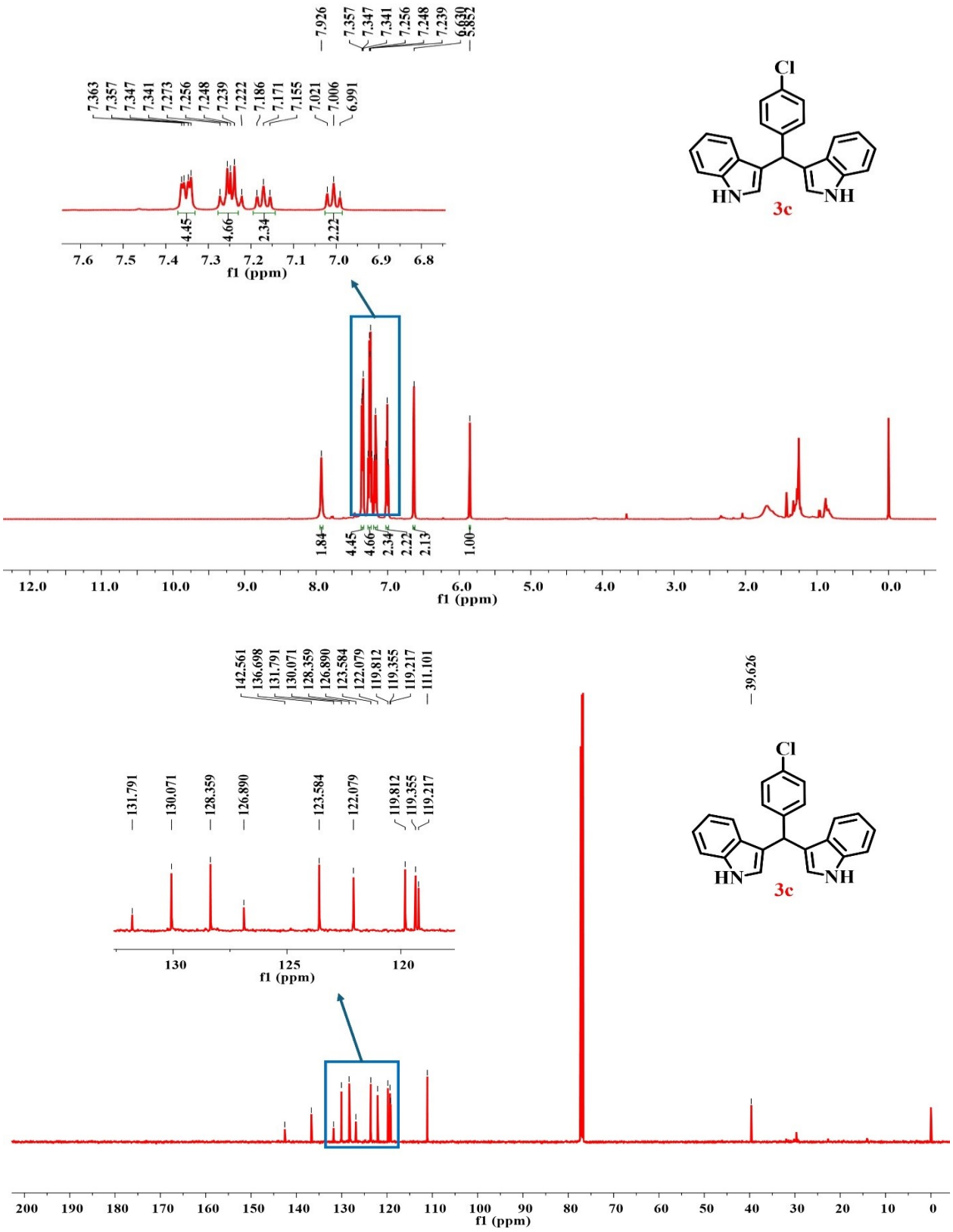

4-(Di(1H-indol-3-yl)methyl)benzonitrile (3d) Dark red solid (94%); mp: 107- 110 °C; ^{1}H NMR (400 MHz, $CDCl_3$) δ 7.98 (s, 2H, NH), 7.55 (d, *J* = 6.8 Hz, 2H, ArH), 7.44 (d, *J* = 6.4 Hz, 2H, ArH), 7.36 (d, *J* = 6.4 Hz, 2H, ArH), 7.32 (d, *J* = 6.4 Hz, 2H, ArH), 7.17 (t, *J* = 6.0 Hz, 2H, ArH), 7.01 (t, *J* = 8.0, 7.1, 0.9 Hz, 2H, ArH), 6.65 (s, 2H, ArH), 5.93 (s, 1H, $(Ar)_3CH$). ^{13}C NMR (100 MHz, $CDCl_3$) δ 149.79, 136.68, 132.16, 129.50, 126.69, 123.64, 122.30, 119.58, 119.56, 119.16, 118.24, 111.23, 110.03, 40.09. HRMS (ESI) calcd for $C_{24}H_{17}N_3$ $[M-H]^-$ 346.1338, found $[M-H]^-$ 346.1337.

Fig. S5(d) ^{1}H and ^{13}C NMR spectra of 4-(di(1H-indol-3-yl)methyl)benzonitrile **(3d).**

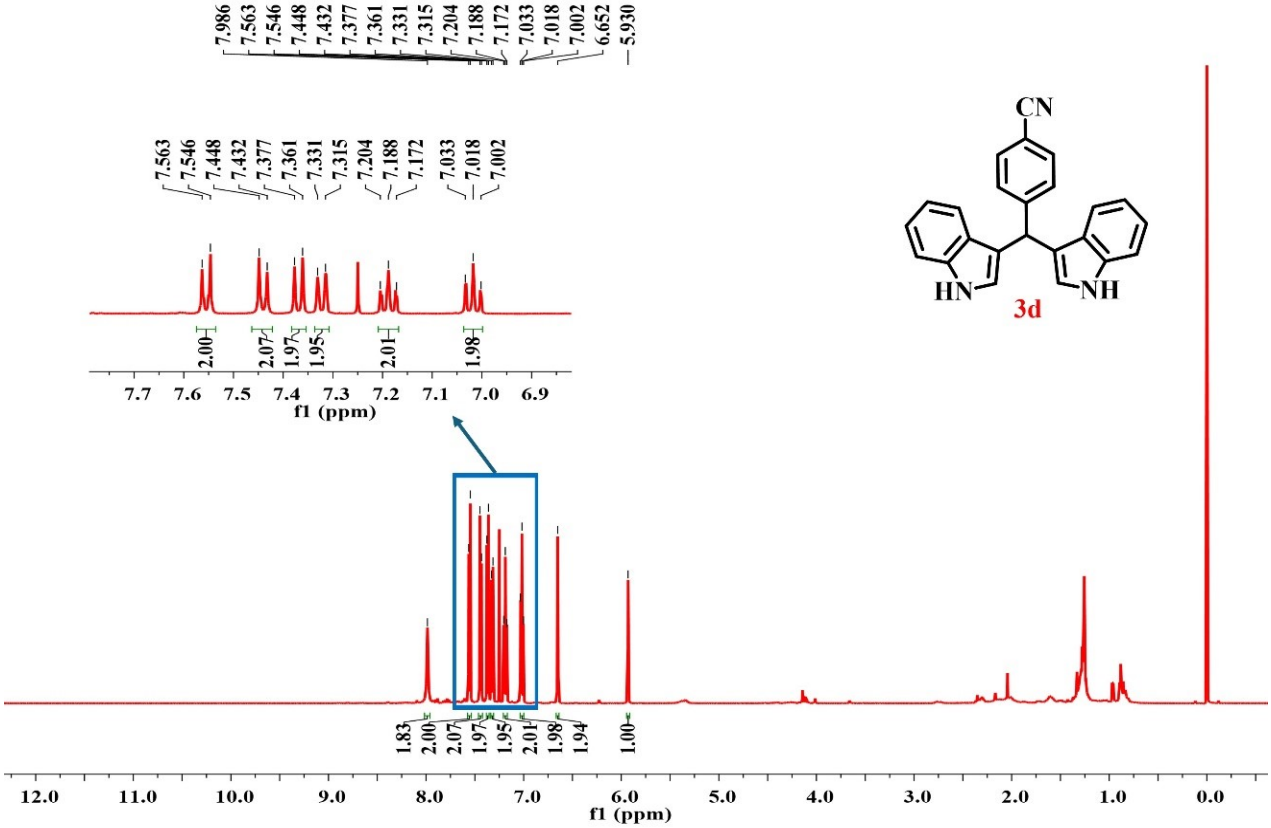

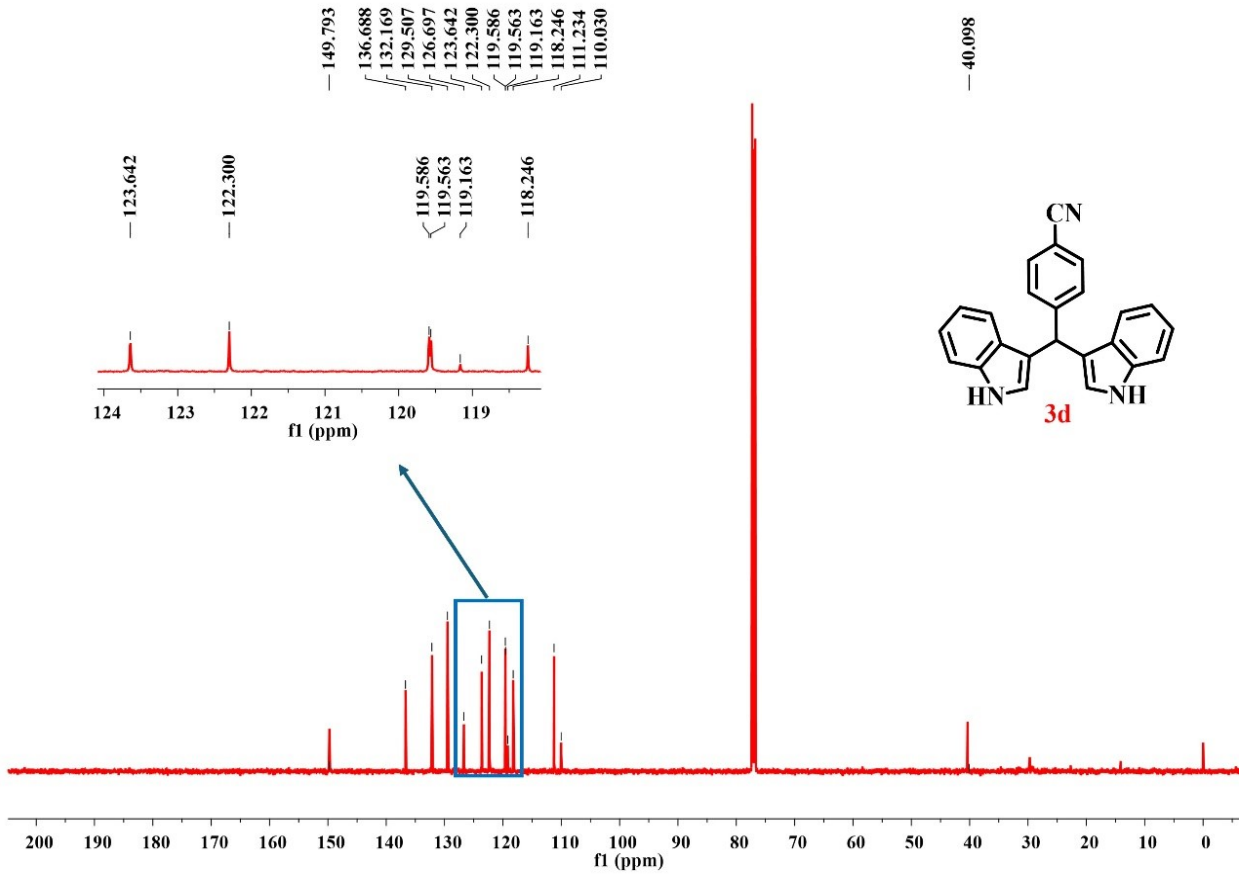

3,3'-((4-Nitrophenyl)methylene)bis(1H-indole) (3e): Yellow solid (76%); mp: 234-236°C; ^{1}H NMR (400 MHz, $CDCl_3$) δ 8.14 (d, *J* = 7.04 Hz, 2H, ArH), 8.00 (s, 2H, NH), 7.50 (d, *J* = 6.8 Hz, 2H, ArH), 7.38 (d, *J* = 6.56 Hz, 2H, ArH), 7.33 (d, *J* = 6.4 Hz, 2H, ArH), 7.20 (t, *J* = 6.52 Hz, 2H, ArH), 7.03 (t, *J* = 6.02 Hz, 2H, ArH), 6.68 (s, 2H, ArH), 5.99 (s, 1H, $(Ar)_3CH$). ^{13}C NMR (100 MHz, $CDCl_3$) δ 151.84, 146.58, 136.70, 129.53, 126.66, 123.63, 122.37, 119.63, 119.57, 118.16, 111.26, 40.21. HRMS (ESI) calcd for $C_{24}H_{17}N_3$ $[M-H]^-$ 366.1237, found 366.0558.

Fig. S5(e) ^{1}H and ^{13}C NMR spectra of **3,3'-((4-nitrophenyl)methylene)bis(1H-indole) (3e).**

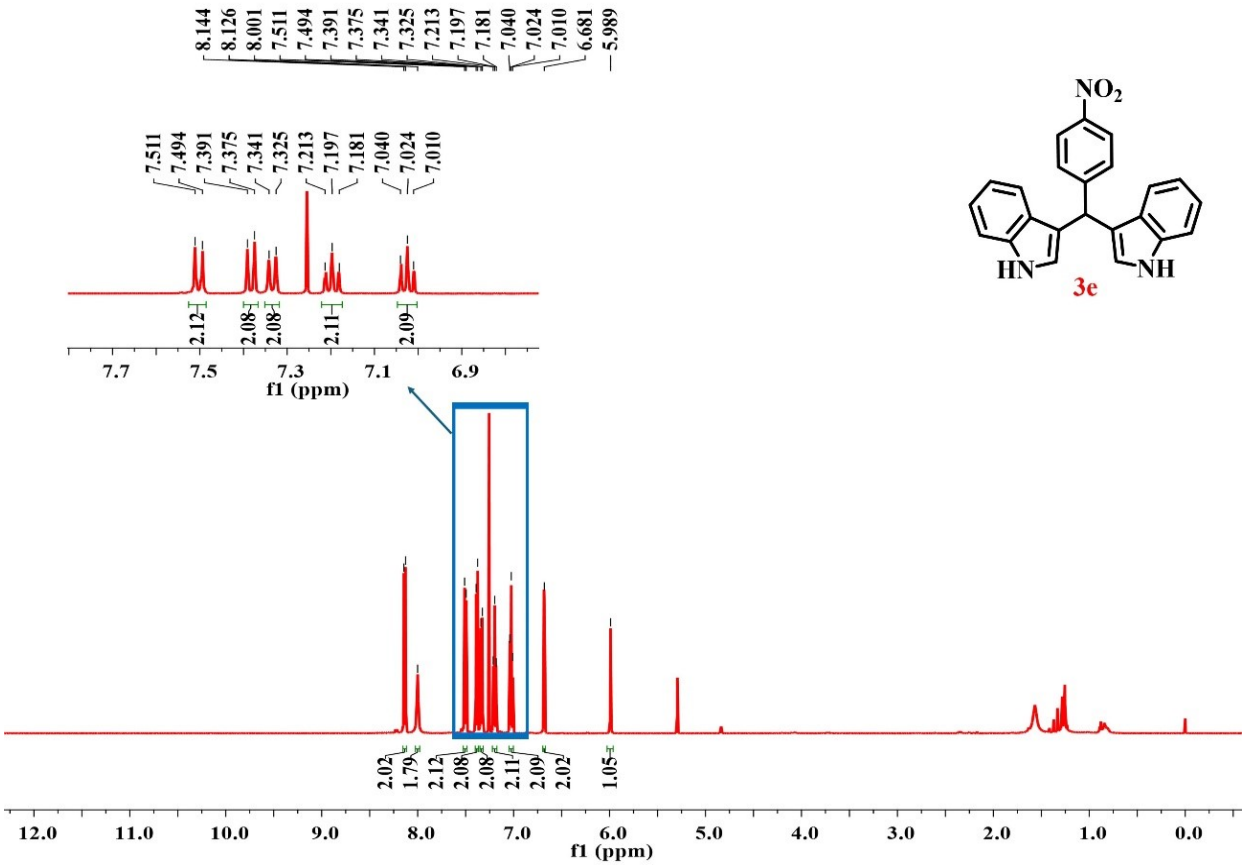
8.144
8.126
8.001
7.511
7.494
7.391
7.375
7.341
7.325
7.213
7.197
7.181
7.040
7.024
7.010
6.681
5.989
NO2
HN
NH
3e
2.12
2.08
2.08
2.11
2.09
f1 (ppm)
2.02
1.79
2.12
2.08
2.08
2.11
2.09
2.02
1.05
f1 (ppm)

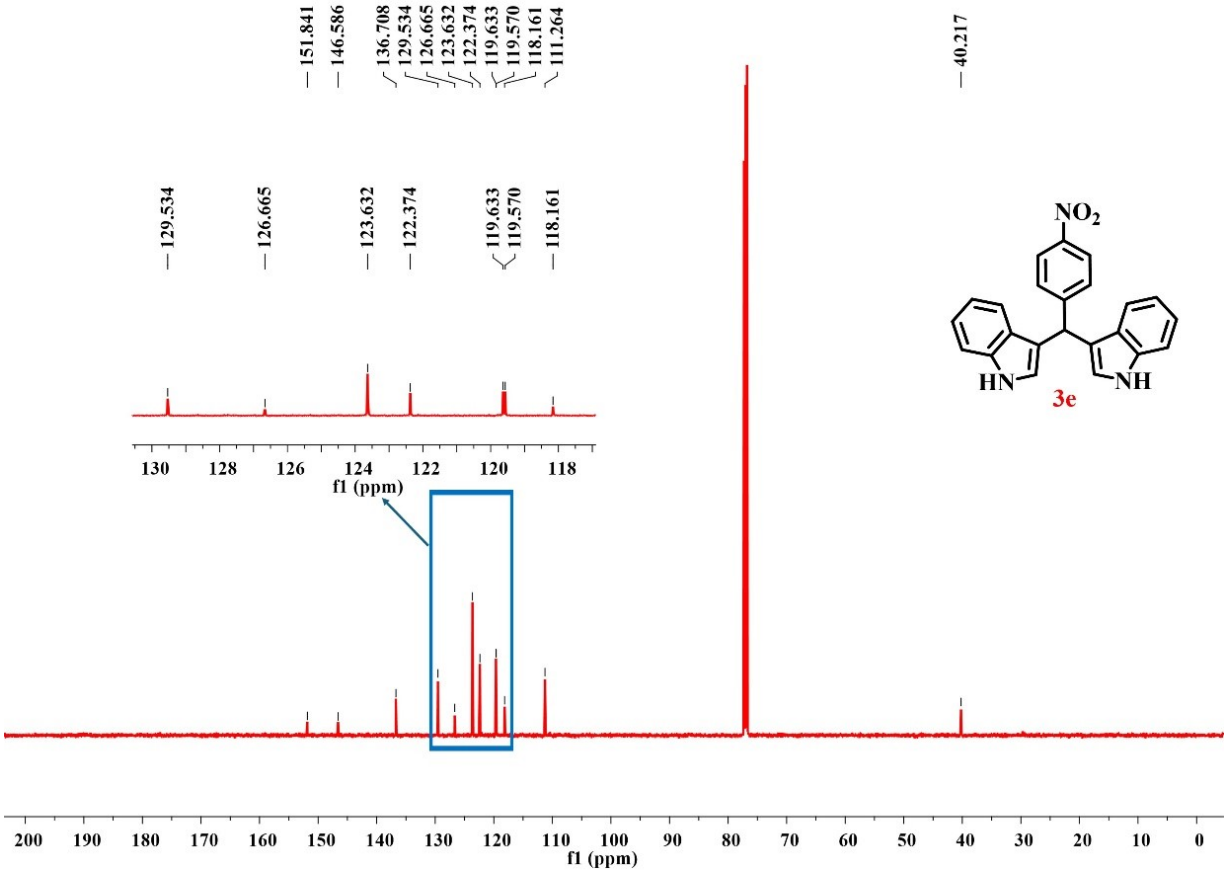
151.841
146.586
136.708
129.534
126.665
123.632
122.374
119.633
119.570
118.161
111.264
40.217
NO2
HN
NH
3e
f1 (ppm)
f1 (ppm)

3,3'-((2-Nitrophenyl)methylene)bis(1H-indole) (3f) Red solid (80 %); mp: 134-138 °C; ^{1}H NMR (500 MHz, $CDCl_3$) δ 7.92 (s, 2H, NH), 7.82 (d, J = 7.0 Hz, 1H, ArH), 7.39 (t, J = 6.1 Hz, 4H, ArH), 7.32 (d, J = 6.5 Hz, 3H, ArH), 7.16 (t, J = 5.7 Hz, 2H, ArH), 7.00 (t, J = 6.0 Hz, 2H, ArH), 6.66 (s, 1H, ArH), 6.62 (s, 2H). ^{13}C NMR (100 MHz, $CDCl_3$) δ 149.76, 137.99, 136.60, 132.30, 131.07, 127.18, 126.75, 124.35, 123.81, 122.14, 119.72, 119.67, 119.53, 117.64, 111.14, 34.35. HRMS (ESI) calcd for $C_{24}H_{17}N_3$ $[M-H]^-$ 366.1237, found $[M-H]^-$ 366.0558.

Fig. S5(f) ^{1}H and ^{13}C NMR spectra of 3,3'-((2-nitrophenyl)methylene)bis(1H-indole) **(3f).**

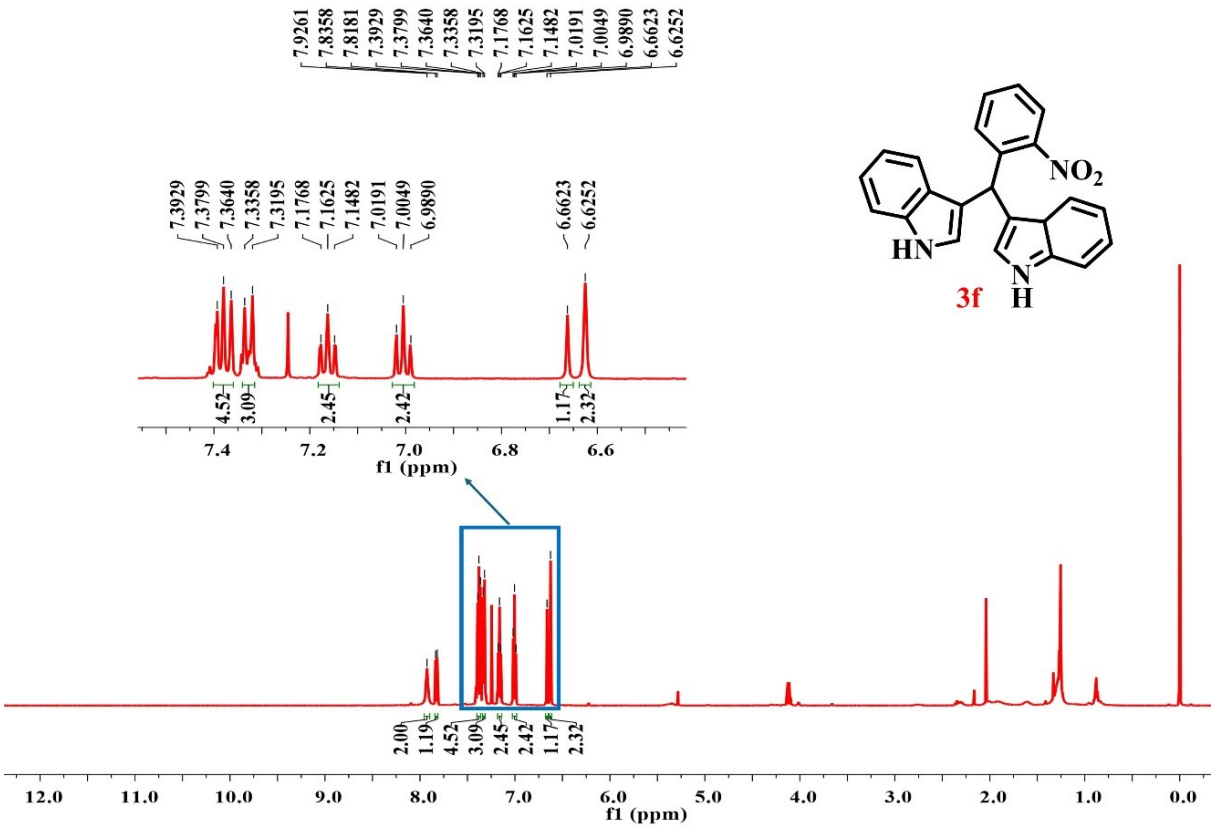

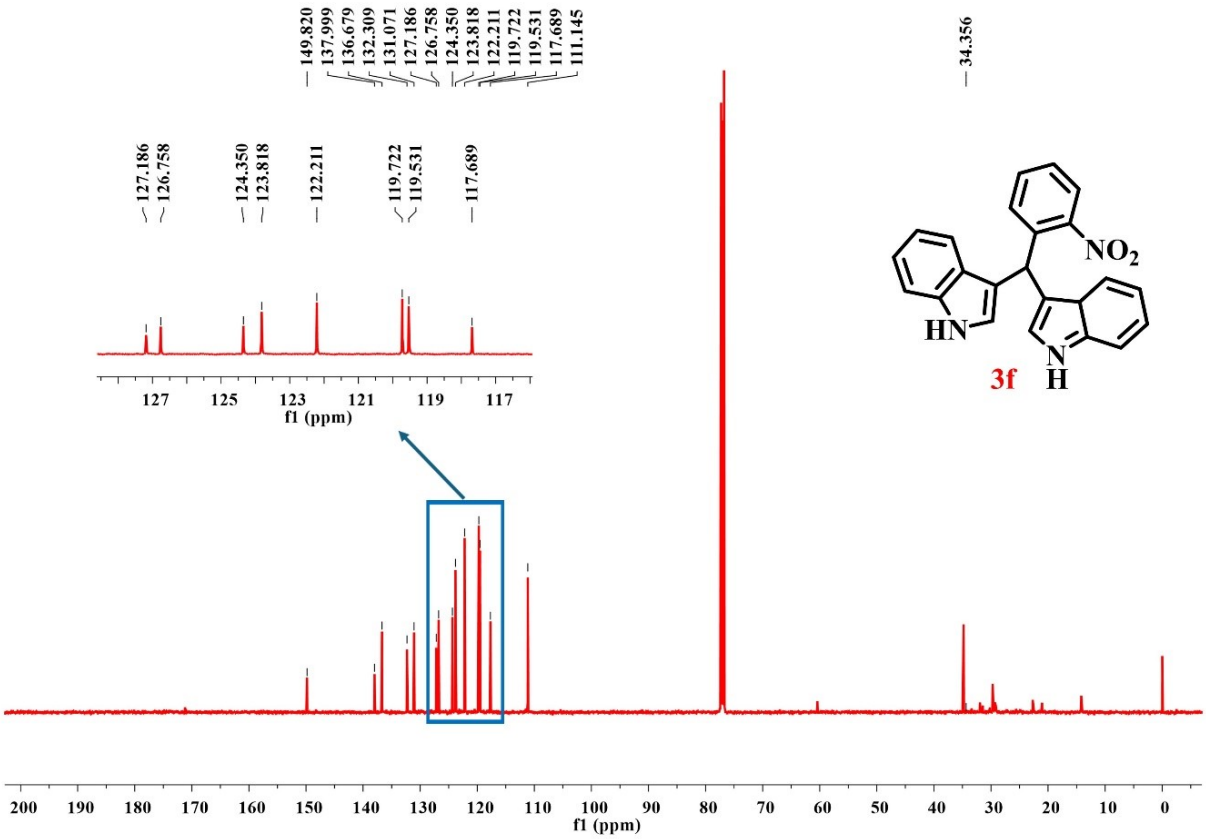

3,3'-((3,4-Difluorophenyl)methylene)bis(1H-indole) (3g) Dark red solid (90%); mp: 96-98 °C; ^{1}H NMR (400 MHz, $CDCl_3$) δ 7.91 (s, 2H, NH), 7.35 (d, J = 6.8 Hz, 4H, ArH), 7.18 (t, J = 6.4 Hz, 2H, ArH), 7.10 (t, J = 7.6 Hz, 1H, ArH), 7.05 – 7.0 (m, 4H, ArH), 6.62 (s, 2H, ArH), 5.83 (s, 1H, $(Ar)_3CH$). ^{13}C NMR (100 MHz, $CDCl_3$) δ 136.69, 126.76, 124.37, 123.52, 122.16, 119.68, 119.43, 118.90, 117.51, 117.37, 116.85, 16.71, 111.16, 39.72. HRMS (ESI) calcd for $C_{23}H_{16}F_2N_2$ $[M-H]^-$ 357.1197, found 357.1201.

Fig. S5(g) ^{1}H and ^{13}C NMR spectra of 3,3'-((3,4-difluorophenyl)methylene)bis(1H-indole) **(3g).**

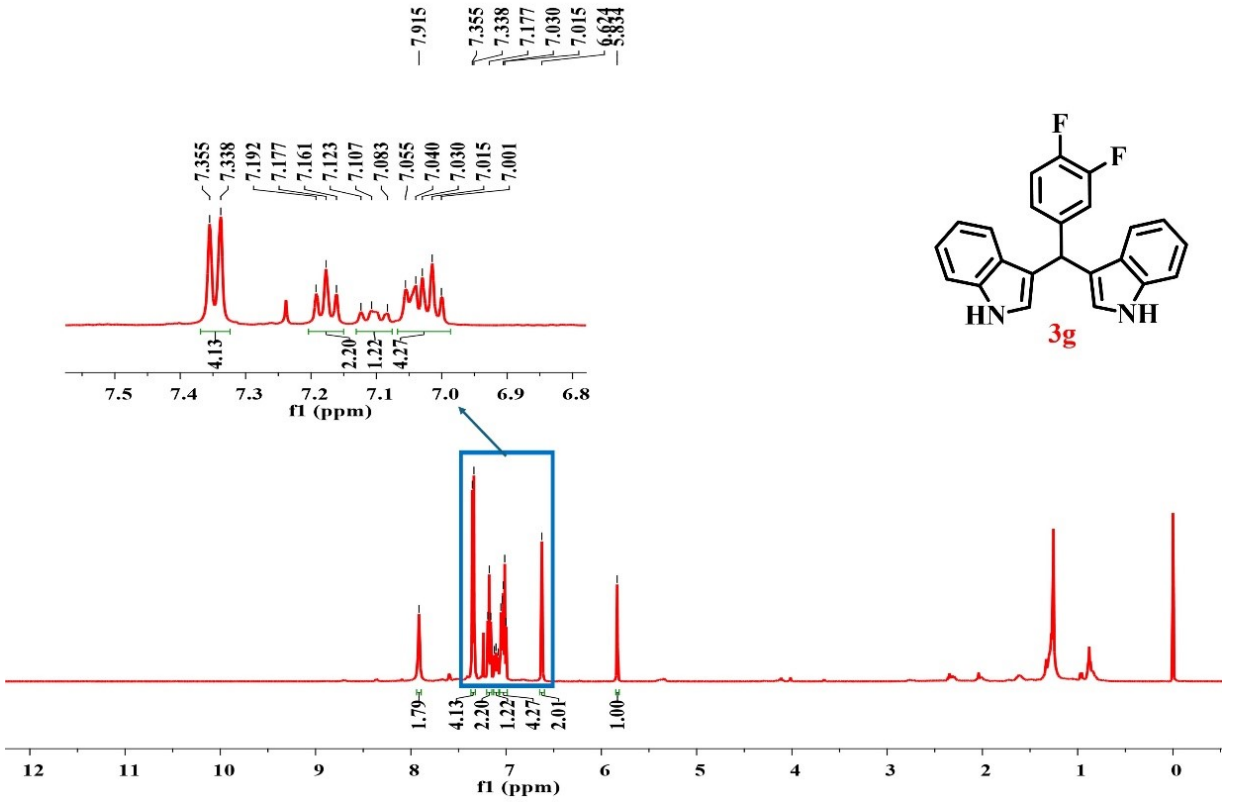
7.915
7.355
7.338
7.177
7.030
7.015
6.624
5.834
7.355
7.338
7.192
7.177
7.161
7.123
7.107
7.083
7.055
7.040
7.030
7.015
7.001
4.13
2.20
1.22
4.27
7.5 7.4 7.3 7.2 7.1 7.0 6.9 6.8
f1 (ppm)
F
F
HN
NH
3g
1.79
4.13
2.20
1.22
4.27
2.01
1.00
12 11 10 9 8 7 6 5 4 3 2 1 0
f1 (ppm)

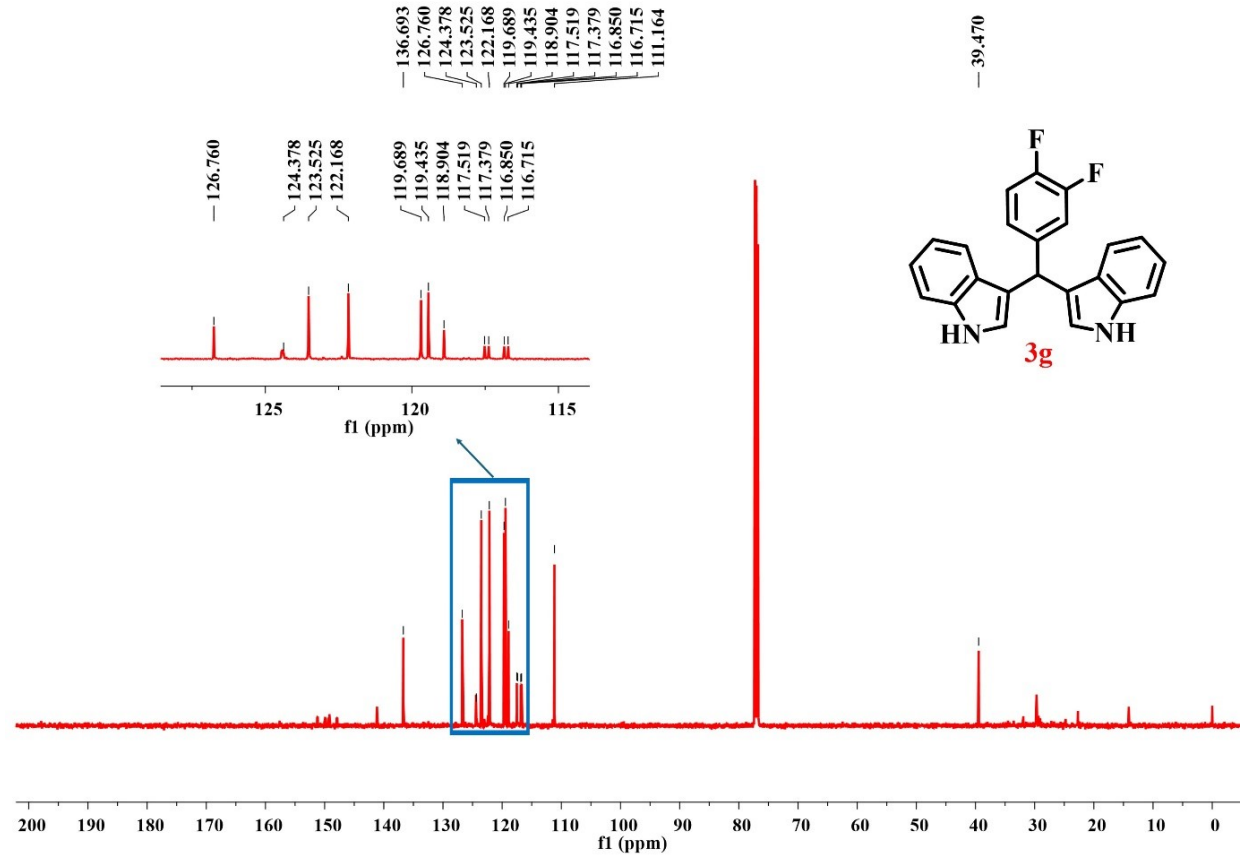
136.693
126.760
124.378
123.525
122.168
119.689
119.435
118.904
117.519
117.379
116.850
116.715
111.164
39.470
126.760
124.378
123.525
122.168
119.689
119.435
118.904
117.519
117.379
116.850
116.715
125 120 115
f1 (ppm)
F
F
HN
NH
3g
200 190 180 170 160 150 140 130 120 110 100 90 80 70 60 50 40 30 20 10 0
f1 (ppm)

3,3'-((2,3-Dichlorophenyl)methylene)bis(1H-indole) (3h) Red solid (72%); mp: 98 – 103 °C; ^{1}H NMR (400 MHz, $CDCl_3$) δ 7.92 (s, 2H, NH), 7.38 (s, 1H, ArH), 7.36 (d, J = 2.2 Hz, 2H, ArH), 7.35 – 7.32 (m, 2H, ArH), 7.17 (t, J = 6.6 Hz, 2H, ArH), 7.13 (dd, J = 7.8, 1.6 Hz, 1H, ArH), 7.05 – 7.00 (m, 3H, ArH), 6.61 (s, 2H), 6.36 (s, 1H, $(Ar)_3CH$). ^{13}C NMR (100 MHz, $CDCl_3$) δ 143.80, 136.71, 133.06, 132.28,128.44, 128.38, 126.89, 126.86, 123.79, 122.14, 119.74, 119.42, 117.91, 111.11, 37.69. HRMS (ESI) calcd for $C_{23}H_{16}Cl_2N_2$ $[M-H]^-$ 389.0606, found 389.0609.

Fig. S5(h) ^{1}H and ^{13}C NMR spectra of 3,3'-((2,3-dichlorophenyl)methylene)bis(1H-indole) **(3h).**

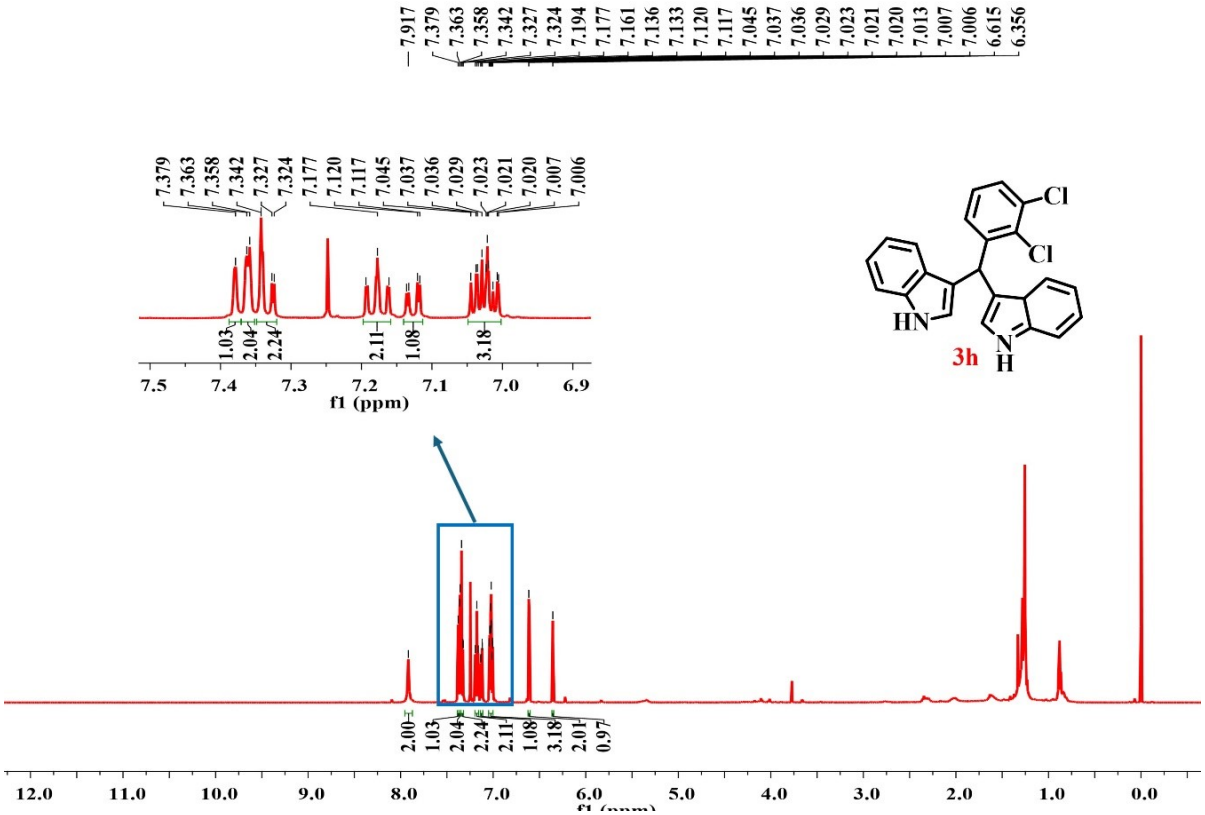

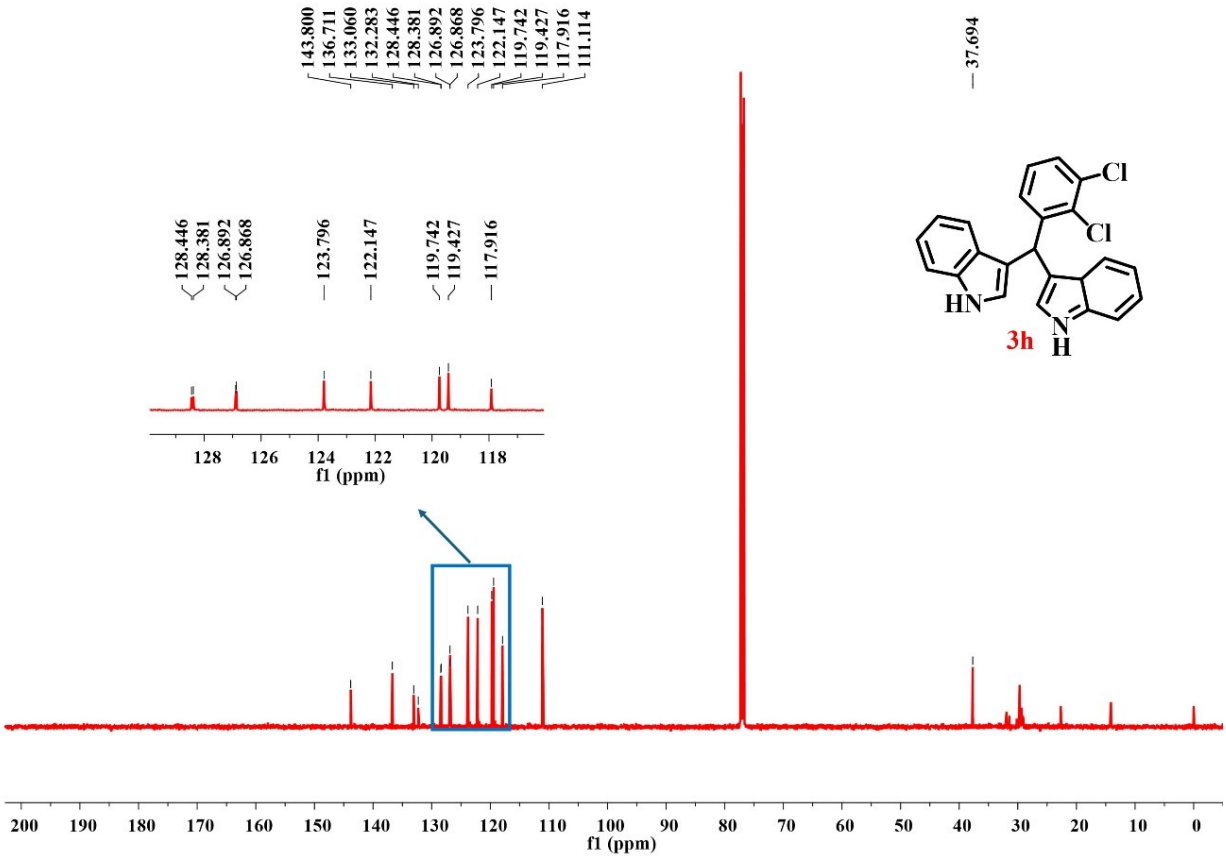

3-(Di(1H-indol-3-yl)methyl)-2-methoxyphenol (3i) Red solid (44%); mp: 128 – 130 °C; ^{1}H NMR (400 MHz, $CDCl_3$) δ 7.83 (s, 2H, NH), 7.37 (d, *J* = 6.3 Hz, 2H), 7.31 (d, *J* = 6.5 Hz, 2H), 7.24 (s, 1H), 7.14 (t, *J* = 6.1 Hz, 2H), 6.98 (t, *J* = 6.0 Hz, 2H), 6.80 (d, *J* = 6.9 Hz, 2H), 6.60 (s, 2H), 5.82 (s, 1H, $(Ar)_3CH$), 3.76 (s, 3H). ^{13}C NMR (100 MHz, $CDCl_3$) δ 157.89, 136.69, 136.23, 129.59, 127.06, 123.50, 121.87, 120.03, 119.97, 119.18, 113.56, 111.00, 55.19, 39.32. HRMS (ESI) calcd for $C_{24}H_{20}O_2N_2$ $[M+H]^+$ 369.1603, found $[M+H]^+$ 369.1595.

Fig. S5(i) ^{1}H and ^{13}C NMR spectra of 3-(di(1H-indol-3-yl)methyl)-2-methoxyphenol **(3i).**

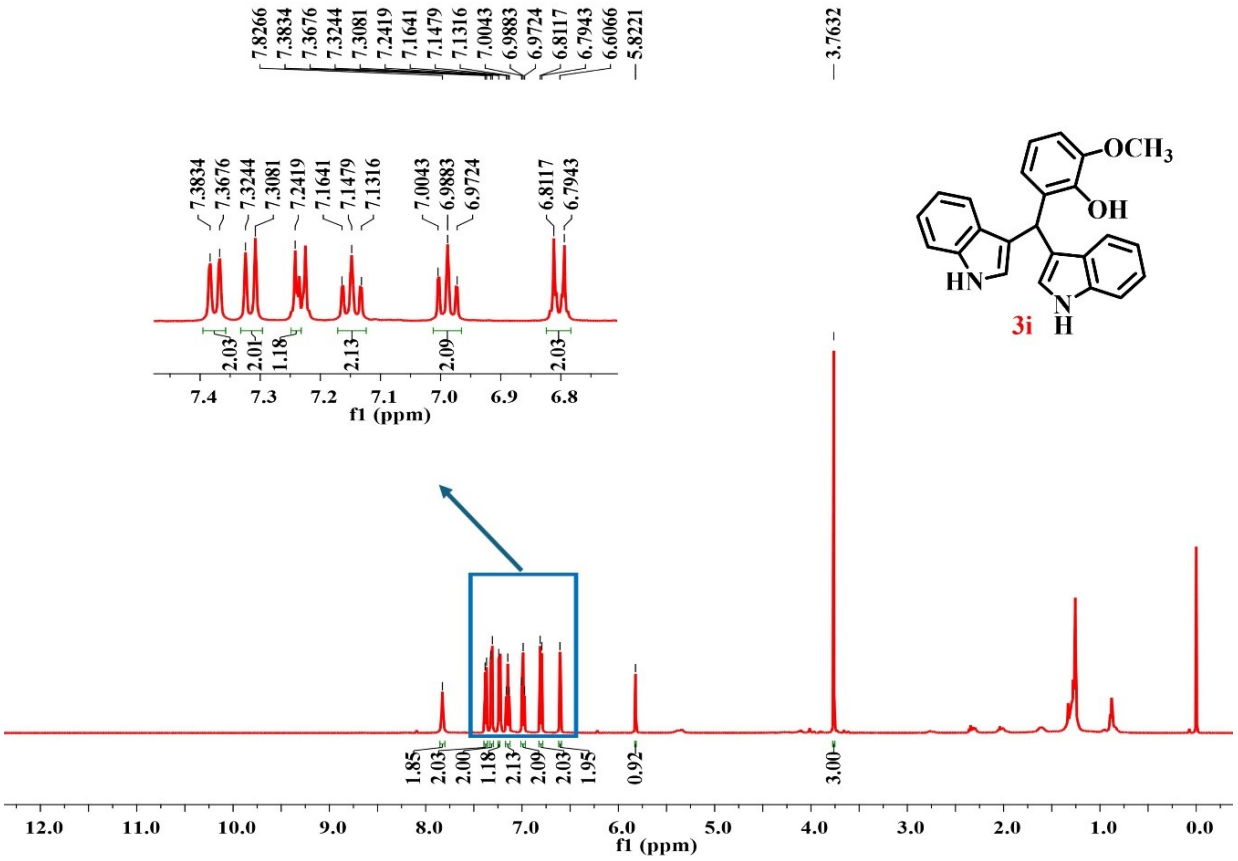
7.8266
7.3834
7.3676
7.3244
7.3081
7.2419
7.1641
7.1479
7.1316
7.0043
6.9883
6.9724
6.8117
6.7943
6.6066
5.8221
3.7632
OCH3
OH
HN
N
H
3i
2.03
2.01
1.18
2.13
2.09
2.03
f1 (ppm)
1.85
2.03
2.00
1.18
2.13
2.09
2.03
1.95
0.92
3.00
f1 (ppm)

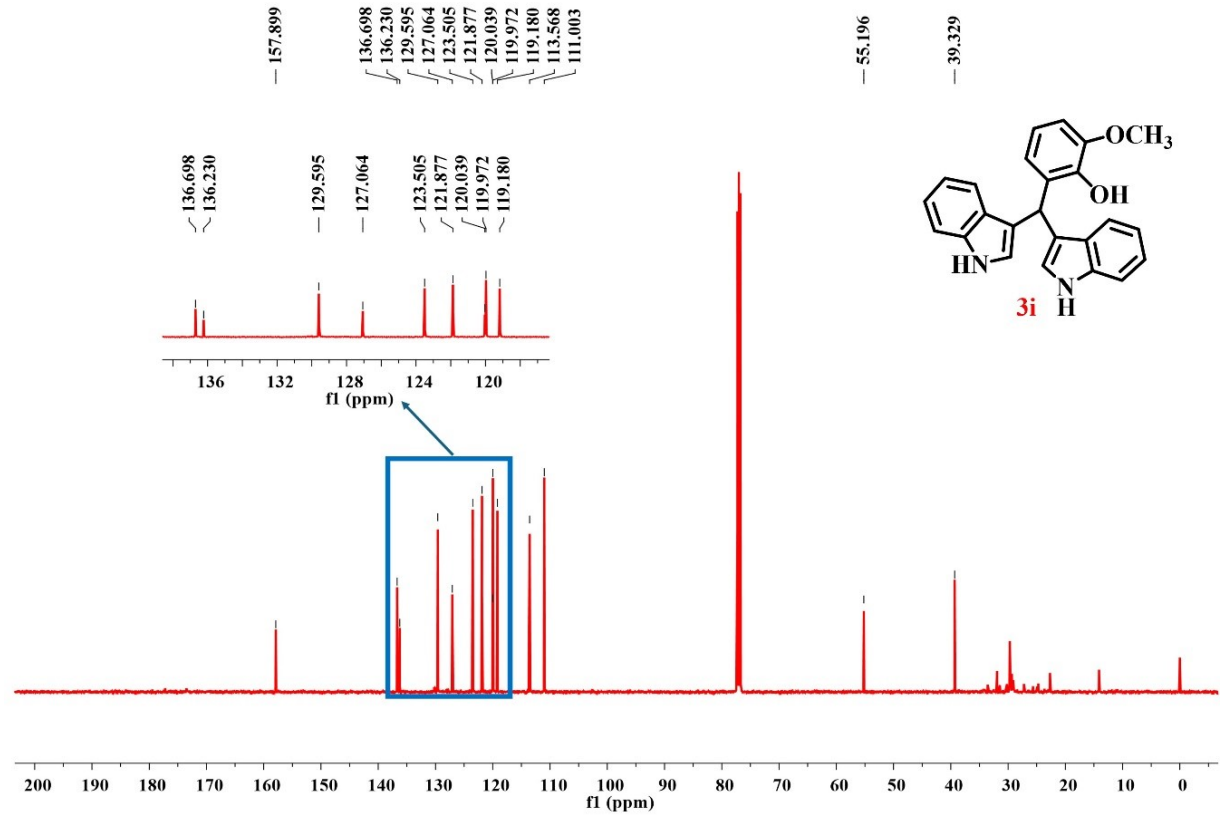
157.899
136.698
136.230
129.595
127.064
123.505
121.877
120.039
119.972
119.180
113.568
111.003
55.196
39.329
OCH3
OH
HN
N
H
3i
f1 (ppm)
f1 (ppm)

Di(1H-indol-3-yl)methane (Arundine) (3j) White solid (66 %); mp: 166-168 °C; ^{1}H NMR (400 MHz, $CDCl_3$) δ 7.84 (s, 1H, NH), 7.62 (d, J = 6.32 Hz, 2H), 7.33 (d, J = 6.52, 2H), 7.18 (t, J = 6.04, 2H), 7.08 (t, J = 5.98 Hz, 2H), 6.90 (s, 2H), 4.23 (t, J = 0.8 Hz, 2H).^{13}C NMR (100 MHz, $CDCl_3$) δ 136.46 (s), 127.57 (s), 122.19 (s), 121.88 (s), 119.22, 119.17, 115.69, 111.03, 29.69, 21.19. HRMS (ESI) calcd for $C_{17}H_{14}N_2$ $[M-H]^-$ 245.1073, found 245.1073.

Fig. S5(j) ^{1}H and ^{13}C NMR spectra of di(1H-indol-3-yl)methane **(3j).**

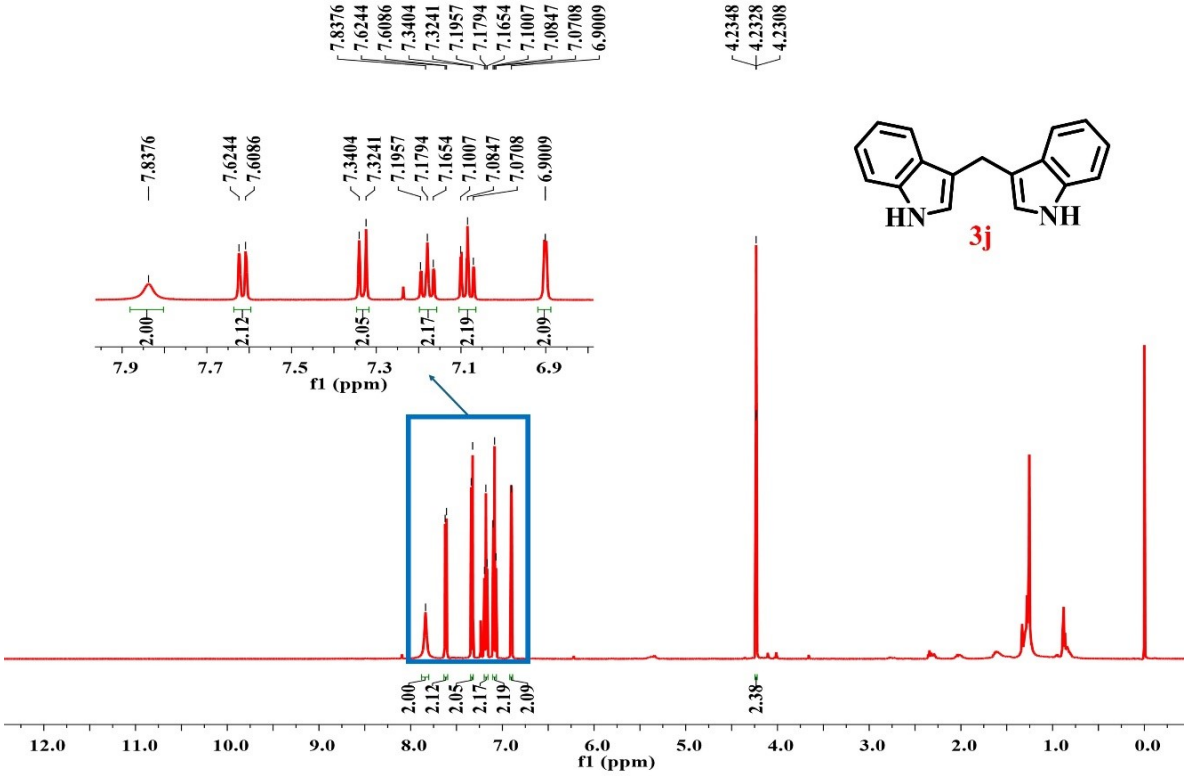

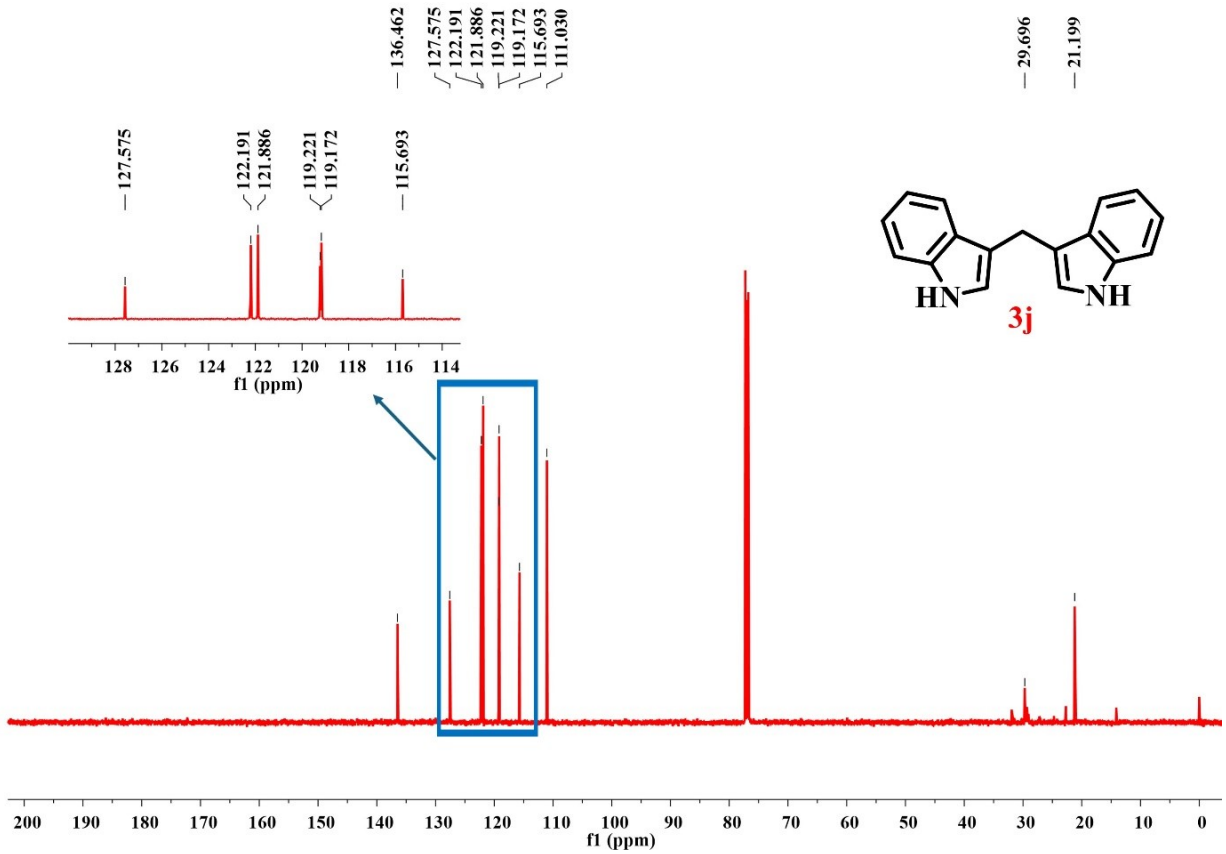

S6. Poisoning experiment

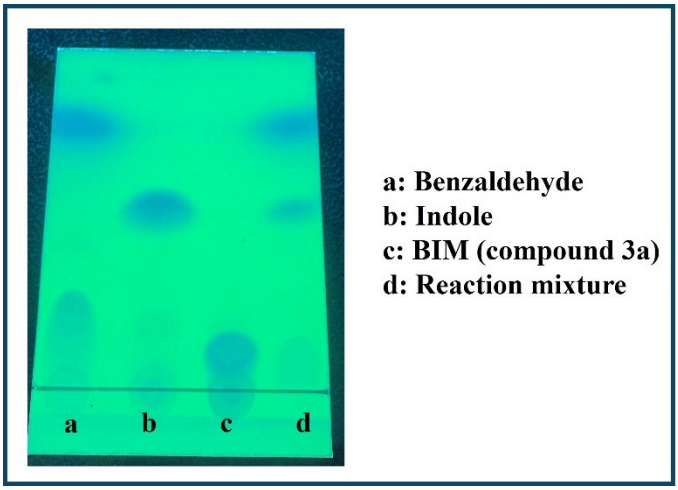

Fig. S6 TLC of poisoning experiment: (a) Benzaldehyde (Reactant), (b) Indole (Reactant), (c) BIM (compound 3a) and (d) reaction mixture from the NH_4OH-poisoned catalyst, showing no spot corresponding to (c), confirming the absence of product formation.

S7. Recycling Studies: Characterization of the recycled ZA2/30 sample using XRD and FE-SEM

The recycled ZA2/30 catalyst obtained after the synthesis of BIM (compound 3a) was characterized using FE-SEM and EDX to evaluate its structural integrity. The detailed recycling procedure is described in the Materials and Methods section (2.7.1), and the corresponding results are discussed in Section 3.7 of the manuscript.

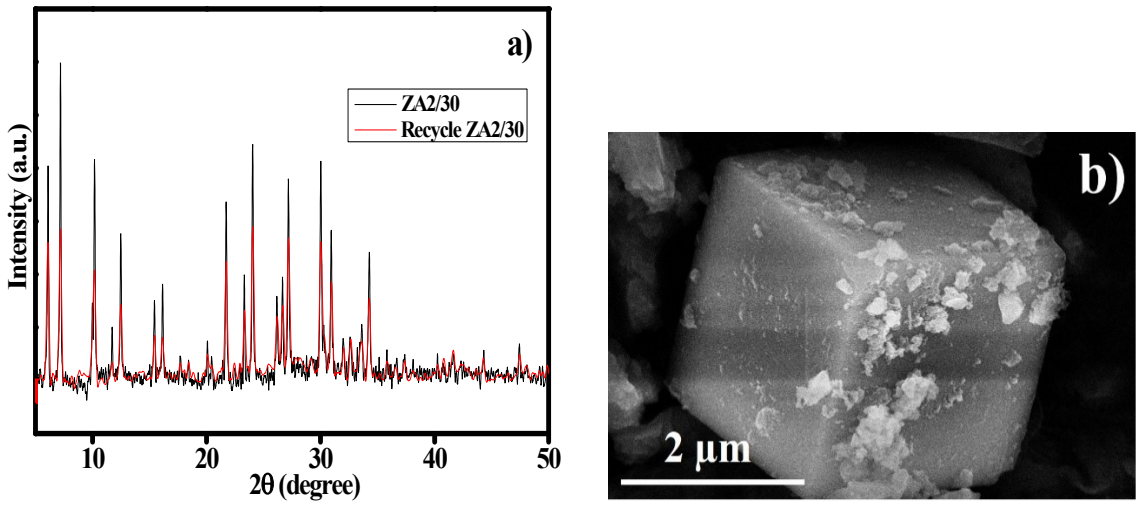

Fig. S7 Characterization of recycled ZA2/30: (a) XRD pattern of recycle ZA2/30 shows a slight decrease in peak intensity compared to fresh ZA2/30; (b) FE-SEM image of recycled ZA2/30 confirms the retention of cubic morphology, indicating no significant structural changes after repeated use in BIM synthesis.

S8. Formula: Calculating the Atom Economy, Process Mass Index and E-factor[4,5]

$$\text{Atom Economy (AE)} = \frac{\text{MW of product (BIM)}}{\text{MW of benzaldehyde+ MW of indole}}$$

$$\text{Process Mass Index (PMI)} = \frac{\text{Total mass in a process or process step}}{\text{Mass of isolated product}}$$

where: Total mass in process
mass of reagents+ mass of solvent

$$\text{E- factor} = \frac{\text{Total mass of waste}}{\text{Mass of isolated product}}$$

References:

1 J. Rohilla, S. Thakur, S. Sharma, R. Singh and V. Kaur, *Dalt. Trans.*, 2025, **54**, 3645–3658.

2 K. Wang, W. Cui, Z. Bian, Y. Liu, S. Jiang, Y. Zhou and J. Wang, *Appl. Catal. B Environ.*, 2021, **281**, 119425.

3 M. T. Jayakumari and C. K. Krishnan, *RSC Adv.*, 2024, **14**, 21453–21463.

4 E. R. Monteith, P. Mampuys, L. Summerton, J. H. Clark, U. W. Maes and C. R. Mcelroy, *Green Chem.*, 2020, **22**, 123–135.

5 A. P. Dicks, *J. Chem. Educ.*, 2015, **92**, 1938–1942.